

Incorporating graph neural network into route choice model

Ma Yuxun^{a,1}, Toru Seo^a

^a*Department of Civil and Environmental Engineering, Institute of Science Tokyo
, 2-12-1-M6-10, Meguro, Ookayama, 152-8552, Tokyo, Japan*

Abstract

Route choice models are one of the most important foundations for transportation research. Traditionally, theory-based models have been utilized for their great interpretability, such as logit models and Recursive logit models. More recently, machine learning approaches have gained attentions for their better prediction accuracy. In this study, we propose novel hybrid models that integrate the Recursive logit model with Graph Neural Networks (GNNs) to enhance both predictive performance and model interpretability. To the authors' knowledge, GNNs have not been utilized for route choice modeling, despite their proven effectiveness in capturing road network features and their widespread use in other transportation research areas. We mathematically show that our use of GNN is not only beneficial for enhancing the prediction performance, but also relaxing the Independence of Irrelevant Alternatives property without relying on strong assumptions. This is due to the fact that a specific type of GNN can efficiently capture multiple cross-effect patterns on networks from data. By applying the proposed models to one-day travel trajectory data in Tokyo, we confirmed their higher prediction accuracy compared to the existing models.

Keywords: Route choice model, Hybrid model, Graph Convolution Network, Recursive logit model, Model interpretability

1. Introduction

Understanding and predicting how travelers choose routes based on road network characteristics is essential for transportation research and practice. With advancements in positioning systems, there is now an increasing amount of travel trajectory data available for route choice modeling. The increased quantity of such data has also enabled the application of big data techniques in this research area.

The most common approach for route choice modeling is the logit model (Ben-Akiva et al., 2004), and its extensions, such as the Recursive logit model (RL) (Fosgerau et al., 2013). They are based on the Random Utility Maximization (RUM) theory, which assumes that travelers consistently choose routes that maximize their expected utility based on given utility functions. These theory-based route choice models offer high interpretability, as they assume that the utility function has a predefined and interpretable form. For example, the value of time can be inferred from the weight of the time component in a linear utility function that includes time and other route attributes.

However, standard logit-type models face several challenges. First, their utility functions are predefined, meaning the models' accuracy heavily depends on the modeler's prior knowledge,

which can limit its ability to capture the complex patterns inherent in real-world route choice behavior. Second, these models exhibit the Independence of Irrelevant Alternatives (IIA) property. Although several modified RUM models have relaxed this property, they still rely on strong assumptions on either the scale parameter or the distribution of the random term (e.g., MNP (Yai et al., 1997), Path size logit model (Ben-Akiva and Lerman, 1985), C-logit (Cascetta et al., 1996), Nested RL (Mai et al., 2015)).

Machine learning (ML) has been widely applied to transportation-related problems, such as traffic flow prediction (Cheng et al., 2018; Tang et al., 2019; Fouladgar et al., 2017; Lu et al., 2020), travel speed prediction (Singh et al., 2011; Zou et al., 2022; Ma et al., 2015), signal control (Xiang and Chen, 2015; Vidhate and Kulkarni, 2017; Liang et al., 2019), traffic safety (Ghahremannezhad et al., 2022; Thaduri et al., 2021), and autonomous driving (Xu et al., 2020; Du et al., 2020). Furthermore, it has also been utilized to address choice problems within the transportation domain, enabling more efficient decision-making processes under certain conditions (Hagenauer and Helbich, 2017; Li et al., 2018). These models significantly enhance prediction accuracy by capturing variable interactions and do not require prior knowledge of the underlying utility functions. However, the result of elasticity analysis showed that ML-based choice models may result in unrealistic behavior. Also, most of machine learning methods are black-box models, which can result in poor interpretability.

Recent studies have started to integrate logit models with deep learning models to capture the complex relationships among variables while maintaining the output rationality of discrete choice models (Han et al., 2020; Sifringer et al., 2020; Wong and Farooq, 2021; Phan et al., 2022). These models have shown their capability to achieve a strong balance between accuracy and interpretability, particularly in mode choice analysis and other transportation applications. These approaches could be further sophisticated by integrating the state-of-art ML methodology.

One of the most significant advancement in ML domain is Graph Neural Networks (GNNs), which can capture spatial dependencies between nodes. Since a road network can be represented by a graph, GNNs are applied to problems in transportation research, including traffic flow prediction (He et al., 2023; Bai et al., 2020; Song et al., 2020), travel time prediction (Lu et al., 2019; Xie et al., 2020) and signal control (Zhong et al., 2021; Hu et al., 2020). However, to the best of the authors' knowledge, there is no existing research has incorporated GNNs into route choice models since most ML-based route choice models are path-based.

The objective of this paper is to develop hybrid route choice models for large-scale networks. The proposed models incorporates GNNs into RL to maintain both the high prediction accuracy of deep learning methods and high interpretability of RL. Furthermore, we show that GNNs can relax the IIA property without introducing strong assumptions. The effectiveness of proposed models is evaluated using real-world dataset.

The contribution of this paper can be summarized as follows:

- We propose hybrid route choice models, termed *ResDGCN-RL* and *ResDGCN2-RL*, that combine RL and GNNs. To the best of the authors' knowledge, this is the first attempt to use GNNs for route choice modeling.
- Given that route choice behaviors inherently depend on the road network structure, use of GNNs would be advantageous. We clarify these advantages theoretically and empirically.
- The proposed models can incorporate predefined interpretable utility functions and non-structured NN functions to enhance accuracy. The balance between these two is adjustable by an exogenous parameter.

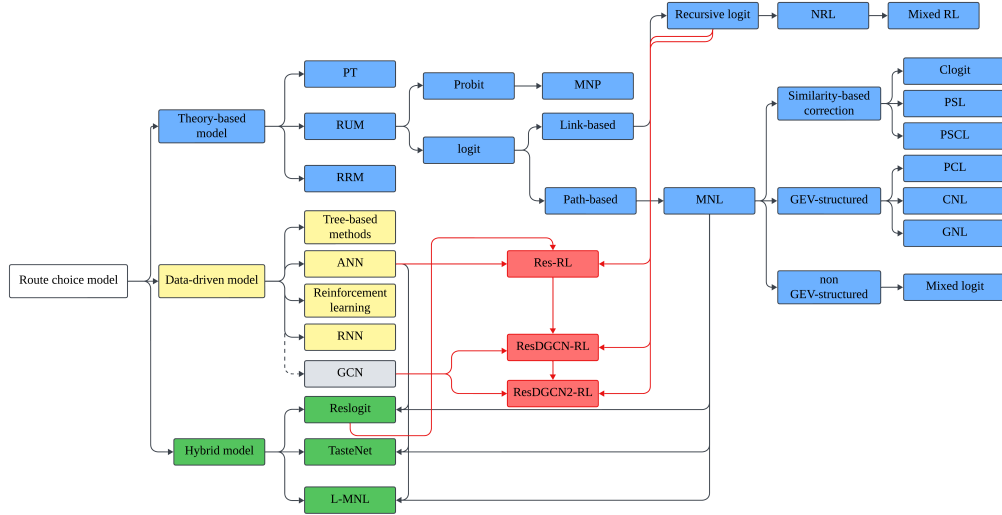


Figure 1: Conceptual framework of the literature review: research gaps and study positioning. This framework highlights existing research gaps, indicated by dotted lines, and emphasizes the focus of this study, represented by red lines and blocks.

- The proposed models relax the IIA property and automatically learn the cross-effect patterns from data.
- To make the above contribution, we propose a novel NN framework.
- Empirical evaluation using real-world data demonstrates the advantages of the proposed models over existing approaches.

The rest of this paper is organized as follows. Section 2 provides an overview of theory-based and data-driven route choice models. Section 3 presents the specification and properties of our proposed models. Section 4 demonstrates proposed models with a very simple network. Section 5 evaluates the performance of proposed models using real vehicle trajectory data in Tokyo. Section 6 concludes our work and discusses potential future research directions.

2. Literature review

In this section, literatures about theory-based, data-driven route choice model, and hybrid models will be reviewed. Figure 1 shows the conceptual framework of this section, highlighting the research gaps and study positioning.

2.1. Theory-based route choice model

Theory-based route choice models rely on assumptions on decision makers, alternatives, attributes of alternatives, and decision rules.

Decision makers Travelers are assumed to be homogeneous and the interactions between travelers are reflected by their socio-economic variables.

Alternatives Travelers have incomplete information about the available choice set.

Attributes Alternatives are characterized by their attributes. The commonly used attributes are travel time and distance.

Decision rule A decision rule defines how travelers make choices based on the available information..

The most commonly used decision rule is RUM, which assumes that travelers have incomplete information and choose the route with highest utility. Uncertainty must be accounted for due to unobserved attributes and individual-specific heterogeneity. This uncertainty is incorporated into the utility function through a random term:

$$U_{in} = V_{in} + \epsilon_{in} \quad (1)$$

where U_{in} means the utility of individual n on choosing alternative i , V_{in} is the systematic part of the utility, and ϵ_{in} is the random term.

The probability of choosing alternative i in choice set C_n can be expressed as:

$$P(i|C_n) = P(U_{in} \geq U_{jn}) \quad \forall j \in C_n \quad (2)$$

Logit model assumes that the random terms follow i.i.d Gumbel distribution (or Type I extreme value) (Gumbel, 1958). The merit of logit model is its tractability. The choosing probability output by Multinomial logit model (MNL) is:

$$P(i|C_n) = \frac{\mu e^{V_i}}{\sum_{j \in C_n} \mu e^{V_j}} \quad (3)$$

where μ is the scale parameter. The IIA property of MNL can be expressed as:

$$\frac{P(i|C_1)}{P(j|C_1)} = \frac{P(i|C_2)}{P(j|C_2)} \quad (4)$$

where C_1 and C_2 are subset of full choice set C_n . The ratio of the two probabilities of two any alternatives does not depends on the utility of other alternatives. However, in route choice problems, the various routes may have overlapping segments, which introduces correlations among the choices. As a result, the IIA property of the logit model can lead to unrealistic outcomes.

Therefore, several modified MNL models are proposed to relax IIA property. Certain models add terms to the utility function to account for the similarity between choices. However, this approach increases model complexity and cannot fully capture the correlation between alternatives. Cascetta et al. (1996) proposed the Clogit model, which introduces a commonality factor into the utility function to capture the similarity between choices and is robust to choice set size. However, the value of the commonality factor depends on the definition of route length and the value of the parameter, and it only captures part of the similarity. Ben-Akiva and Lerman (1985) proposed the Path-Size Logit (PSL) model, which is easier to compute, but it still only captures part of the similarity. Bovy et al. (2008), inspired by RUM theory, proposed the Path Size Correction Logit model (PSCL), however, the performance of PSCL is sensitive to the choice set.

Generalized Extreme Value (GEV) models are a class of discrete choice models based on the GEV distribution. Prashker and Bekhor (2000) proposed the Paired Combinatorial Logit (PCL) and Cross Nested Logit (CNL) models to solve the stochastic user equilibrium problem.

PCL assumes that travelers always make decisions between pairs of alternatives, while CNL assumes that routes are chosen within a nest. However, the complexity of both models increases with the size of the network. Moreover, Bekhor and Prashker (2001) applied the same idea to the Generalized Nested Logit (GNL) model, where the nesting coefficient is considered a parameterized mean of the inclusion coefficients.

In addition to GEV-based models, several non-GEV models have been developed. Yai et al. (1997) proposed the Multinomial Probit (MNP) model, which assumes that the random term of the utility function follows a normal distribution. A limitation of MNP is the complexity involved in calculating the choice probability. McFadden and Train (2000) proposed the Mixed Logit model, which assumes that the utility function has random coefficients.

Fosgerau et al. (2013) proposed Recursive Logit model which does not require generating choice set before modeling. However, it still suffers from IIA property. Mai et al. (2015) proposed a nested recursive logit model (NRL) by assuming the scale parameters are non-equal among links. Mai et al. (2018) also proposed a mixed recursive logit model by assuming that the parameters in deterministic instantaneous utility are normally distributed. Due to the difficulty in calculating value function, these improved RL models still rely on strong assumption on scale parameters and parameters in utility function.

In addition to RUM theory, other choice theories used in route choice modeling include Prospect Theory (PT) (Zhang and He, 2014) and the Random Regret Minimization Theory (RRM). However, the models based on these theories are often overly complex, which makes model training challenging. Route choice models based on RUM theory are primarily limited by the assumptions on random term and by the approaches used to relax the IIA property.

2.2. *Data-driven route choice model*

With the growth in available data, many studies have begun to adopt data-driven methods for route choice modeling. These approaches have significantly improved prediction accuracy.

One of the earliest studies on route choice was conducted by Yamamoto et al. (2002), who used decision trees to predict travelers' choices between two expressways. Lee et al. (2010) proposed a logistic regression tree to model how travelers choose routes when provided with information. A random forest (RF) is an ensemble learning method that builds multiple decision trees, each using a random subset of variables, and combines their outputs to improve prediction accuracy and reduce overfitting. Tribby et al. (2017) used RF to model pedestrian route choice and found that RF has better prediction accuracy and does not require predefined theoretical constructs. Schmid et al. (2022) compared RF with Multinomial Logit (MNL), Mixed Logit, Artificial Neural Network (ANN), and Support Vector Machine (SVM) and found that RF outperforms these models in prediction accuracy. They also observed that the variable importance ranking differs among RF, MNL, and Mixed Logit. While these tree-based methods offer high interpretability, they generally have lower prediction accuracy compared to more complex models. Furthermore, tree-based methods are limited in that their outputs cannot account for all possible routes.

Neural Networks (NN) can capture the underlying patterns in input data by mimicking the human brain. Most studies that have utilized NN take features as input and route choice probabilities as output. Yang et al. (1993) proposed an NN-based method to model whether travelers will choose the freeway or a side road. Dia and Panwai (2007) employed an agent-based neural network to analyze the relationship between socio-economic, contextual, and informational features and commuter route choice behavior. Other studies have compared NN with other sta-

tistical methods, demonstrating that NN-based models can achieve better performance (Politis et al., 2023; Lai et al., 2019).

Reinforcement learning has been applied to route choice models to learn the optimal policy for selecting the next link. Zhao and Liang (2023) proposed a deep inverse reinforcement learning-based route choice model, assuming that the reward function and policy function are context-dependent. Similar to RL, the proposed model is also link-based. Wei et al. (2014) introduced a day-to-day dynamic route choice model based on reinforcement learning. In fact, RL is a form of Inverse Reinforcement Learning, where the transition probability is 1.

RNN can process sequential data by its internal memory component to save the previous input and output, and accordingly, is always applied in Natural Language Process and time series analysis. By treating route as a sequence of links, RNN can be utilized for route choice. Dong et al. (2022) proposed a utility-based Hybrid Transformer LSTM model to analyze drivers' route choice behavior. Wang et al. (2021) enhanced A^* search algorithm with RNN to realize personal route recommendation.

2.3. Integration of deep learning and discrete choice model

Despite the high prediction accuracy of deep learning methods, the relationship between input and output is very hard to understand and accordingly they are criticized as black box models. Recently, the researches on integrating deep learning and discrete choice model become popular.

Sifringer et al. (2020) integrated Artificial Neural Network (ANN) into MNL and Nested logit. The systematic utility is divided into two subparts which are the knowledge-driven part and data-driven part. The former one can be calculated by a predefined model and the latter one is the output of ANN. The estimation result showed that the proposed hybrid models (L-MNL and L-NL) outperform the traditional model. Wong et al. (2018) integrated restricted Boltzmann machine (RBM) into MNL to represent latent behavior attributes. Han et al. (2020) proposed a TasteNet-MNL that divided systematic utility into two subparts as well. However, in the data-driven part, the output of NN is the parameter of the linear function.

The closest study relative to this study is Reslogit (Wong and Farooq, 2021). Figure 2 shows the framework of a two-layer Reslogit. The utility of choosing alternative i from J alternatives by individual n in a choice task t can be expressed as:

$$U_{int} = V_{int} + g_{int} + \epsilon_{int} \quad (5)$$

where V_{int} and g_{int} is the systematic component and the residual component of U_{int} , respectively, and ϵ_{int} is a random term. Let V_{nt} to be a $J \times 1$ vector where the i -th element is V_{int} which can be calculated by a linear function and g_{nt} to be a $J \times 1$ vector where the i -th element is g_{int} . g_{nt} can be calculated by:

$$g_{nt} = - \sum_{m=1}^M \ln \left(1 + \exp \left(\theta^{(m)} h_{nt}^{(m-1)} \right) \right) \quad (6)$$

where $h_{nt}^{(m)}$ is the m -th hidden layer.

The input layer is the systematic component:

$$h_{nt}^{(0)} = V_{nt} \quad (7)$$

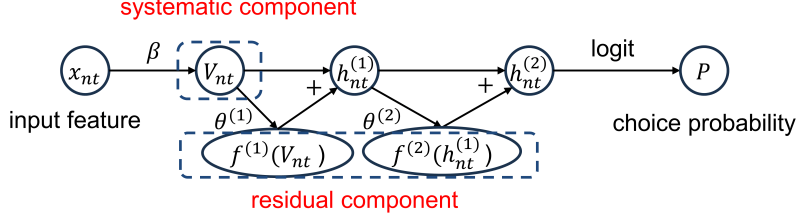


Figure 2: Framework of Reslogit. $f(\cdot)$ represents the propagation rule.

For the m -th block:

$$h_{nt}^{(m)} = h_{nt}^{(m-1)} - \sum_{m'=1}^m \ln(\mathbf{1}_{J \times 1} + \exp(\theta^{(m')} h_{nt}^{(m'-1)})) \quad \forall m \geq 1 \quad (8)$$

where $\mathbf{1}_{J \times 1}$ is a $J \times 1$ all-ones matrix and $\theta^{(m)}$ is a learnable $J \times J$ matrix.

The weight matrices $\theta^{(m)}$ can reflect the cross-effect between alternatives. If they are all identity matrices, there is no cross-effect between alternatives and the Reslogit model is the same as MNL. By using skip connection structure, problem of exploding/vanishing gradient can be avoided during backpropagation.

3. Methodology

In this section, we formulate the proposed hybrid route choice models. First, Res-RL is formulated by simply extending RL following an existing approach (i.e. Reslogit (Wong and Farooq, 2021)). Then, our novel models, termed ResDGCN-RL and ResDGCN2-RL, are formulated by incorporating GNN into RL to capture the graph structure of road network. Among these models, ResDGCN-RL and ResDGCN2-RL represent the key contributions of this work.

3.1. Recursive logit model and its variants

As a preparation, we summarize the existing RL formulation. Consider a road network $G = \langle \mathcal{A}, \mathcal{V} \rangle$ where \mathcal{A} and \mathcal{V} are the sets of nodes and links and A is the adjacency matrix. In RL model, route choice problem is transformed into a sequence of link choice problems. Figure 3 showed a simple road network, where travelers currently at link k , with a destination at d , are assumed to choose the outgoing link a has highest summation of instantaneous utility $u^{\text{RL}}(a|k; \beta)$ and expected maximum downstream utility $V^d(a)$. The instantaneous utility of choosing link a from k can be expressed as:

$$u^{\text{RL}}(a|k; \beta) = v^{\text{RL}}(a|k; \beta) + \mu_k \epsilon(a) \quad (9)$$

where $v^{\text{RL}}(a|k; \beta)$ is a deterministic utility of traveling from link k to a usually calculated by a predefined linear function with parameters β , μ_k is scale parameter for link k and assumed to be the same across all links, and $\epsilon(a)$ are i.i.d extreme type 1 error terms.

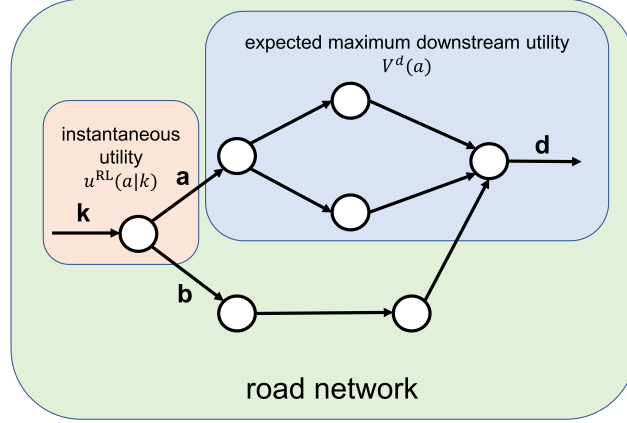


Figure 3: Illustrative road network for Recursive logit model

The expected maximum downstream utility at link a when the destination is d is calculated by Bellman's equation:

$$V^d(a) = \mathbb{E} \left[\max_{a \in A(k)} \frac{1}{\mu_k} (u(a|k) + V^d(a)) \right] \quad (10)$$

where $A(k)$ means the outgoing links of link k and $V^d(d) = 0$. By using logsum, the equation 10 can be expressed in a simpler way:

$$\frac{1}{\mu_k} V^d(a) = \ln \left(\sum_{a \in A(k)} e^{v(a|k) + V^d(a)} \right) \quad (11)$$

Assume that the choice probability of link a at link k with destination d is calculated by an MNL model.

$$P^d(a|k) = \delta(a|k) \frac{e^{v(a|k) + V^d(a)}}{\sum_{a' \in A(k)} e^{v(a'|k) + V^d(a')}} = \delta(a|k) e^{v(a|k) + V^d(a) - V^d(k)} \quad (12)$$

where $\delta(a|k)$ is a dummy variable, equals one if $A(k, a) = 1$.

In order to overcome correlation in error terms due to physical overlapping, Fosgerau et al. (2013) used link flow calculated by predefined parameters as a proxy of link size attribute. This follows a similar rationale to the Path Size logit model in addressing route overlap (Ben-Akiva and Lerman, 1985). Consider a destination d , G^a is a vector of size $|V|$ with the a -th element as 1 and all other elements as 0 and the destination is d , $|V|$ is the number of links. P^d is the choice probability matrix with elements $P^d_{k,a} = P^d(a|k)$. The expected link flow for origin and destination pair od , denoted as F^{od} , can be calculated by:

$$\left(I - (P^d)^T \right) F^{od} = G^o \quad (13)$$

By incorporating the link size attribute into the utility function, we can partially address the IIA problem. However, this approach requires presetting parameters for the utility function and calculating the link size for each OD pair, making it complex.

NRL (Mai et al., 2015) can also solve the physical overlapping problem. The difference between NRL and RL is that the scale parameter μ_k in NRL is not a constant but depends on the characteristics of link.

3.2. Residual Recursive logit model

While the standard RL model effectively captures sequential decision-making in route choice, it cannot capture the complex correlation between alternatives due to its IIA property. Inspired by Reslogit (Wong and Farooq, 2021), we extend RL to a new model called Residual Recursive logit model (Res-RL).

3.2.1. Formulation of Res-RL

The instantaneous utility of choosing link a from k is defined as:

$$u^r(a|k) = v^r(a|k) + g^r(a|k) + \epsilon(a) \quad (14)$$

where $v^r(a|k)$ and $g^r(a|k)$ are systematic component and residual component for choosing link a from k of Res-RL respectively. $\epsilon(a)$ is an i.i.d extreme value type 1 distributed random term. The systematic component is calculated by a linear function of Action adjacency Matrix, denoted by $F_1 \dots F_{D_1}$, where $F_i(k, a)$ is the i -th feature of traveling from link k to a and D_1 is the number of action features.

The residual component is calculated by:

$$G^r = - \sum_{m=1}^M \ln \left(J + \exp \left(h^{r,m-1} \theta^{r,m} \right) \right) \otimes A \quad (15)$$

where G^r is the residual component matrix with elements $G_{k,a}^r = g^r(a|k)$. $h^{r,m}$ is the output of m -th hidden layer, while $\theta^{r,m}$ is a $|V| \times |V|$ weight matrix in m -th hidden layer. In this paper, both $\theta_{i,j}$ and $\theta(i, j)$ refer to the element in the θ matrix at the i -th row and j -th column. M is the total number of hidden layers, J is an all-ones matrix of size $|V| \times |V|$, and \otimes is element-wise product.

For the input layer,

$$h^{r,0} = V^r \quad (16)$$

where V^r is the systematic component matrix with elements $V_{k,a}^r = v^r(a|k)$.

For each hidden layer $h^{r,m}$:

$$h^{r,m} = h^{r,m-1} - \ln \left(J + \exp \left(h^{r,m-1} \theta^{r,m} \right) \right) \otimes A \quad \forall m \geq 1 \quad (17)$$

3.2.2. Property of Res-RL

Similar to Reslogit, Res-RL exhibits two key properties: an interpretable weight matrix and a skip connection mechanism. First, the weight matrix effectively reflects the cross-effects between travel actions. To better understand this property, we define the cross-effect, outgoing link pair, and intersection cross-effect as follows:

Cross-effect The cross-effect between alternatives describes how the utility of one action is influenced by the utility of another action.

Outgoing link pair The outgoing link pair consists of links that share a common node as their origins.

$$\{(v, u) \mid (v, u) \in \mathcal{V}\} \cup \{(v, w) \mid (v, w) \in \mathcal{V}\}$$

Intersection cross-effect The intersection cross-effect represents the cross-effect between the utility of actions that travel from a given link to the links in its outgoing link pair.

The element $\theta_{a',a}^{r,m}$ plays a crucial role in capturing *intersection cross-effects*. It reflects the impact of the utility of traveling to link a' on the of one traveling to link a . In a simple one-layer Res-RL, the utility of traveling from link k to link a is defined as:

$$u^r(a|k) = v^r(a|k) - \ln \left(1 + \exp \left(\sum_{a' \in A(k)} v^r(a'|k) \times \theta_{a',a}^{r,1} \right) \right) + \epsilon(a) \quad (18)$$

The term $\exp(\sum_{a' \in A(k)} v^r(a'|k) \times \theta_{a',a}^{r,1})$ represents how the utilities of choosing other link affect the utility of choosing link a . To quantify this effect, we take the partial derivative of $u^r(a|k)$ with respect to $v^r(a'|k)$ where $a, a' \in A(k)$ and $a \neq a'$:

$$\frac{\partial u^r(a|k)}{\partial v^r(a'|k)} = \frac{\exp(g_{k,a}^r) - 1}{g_{k,a}^r} \theta_{a',a}^{r,1} \quad (19)$$

It is easy to prove that $\frac{\exp(g_{k,a}^r) - 1}{g_{k,a}^r}$ is larger than 0. Accordingly, a positive value of $\theta_{a',a}^{r,1}$ indicates that a higher $v^r(a'|k)$ leads to a higher $u^r(a|k)$, and vice versa. However, while Res-RL effectively captures *intersection cross-effect* via the weight matrix, it does not account for other complex cross-effect pattern.

The second property is skip connection mechanism, originally introduced by He et al. (2016). This mechanism helps Res-RL mitigate the exploding and vanishing gradient problems, ensuring that an increasing number of hidden layers does not degrade performance. The partial derivative of $u^r(a|k)$ with respect to θ is:

$$\begin{aligned} \frac{\partial u^r(a|k)}{\partial \theta} &= \frac{\partial u^r(a|k)}{\partial v^r(a|k)} \times \frac{\partial v^r(a|k)}{\partial \theta} + \frac{\partial u^r(a|k)}{\partial (h^{r,1} - h^{r,0})} \times \frac{\partial (h^{r,1} - h^{r,0})}{\partial \theta} + \dots + \\ &\quad \frac{\partial u^r(a|k)}{\partial (h^{r,M} - h^{r,M-1})} \times \frac{\partial (h^{r,M} - h^{r,M-1})}{\partial \theta} \end{aligned} \quad (20)$$

The equation 20 shows the nature of skip-connection, where the derivative of residual layers is independently computed. Each term in the summation corresponds to an independent gradient path, meaning that even if one term approaches zero, the total gradient remains nonzero, allowing effective learning.

In contrast, if the residual connection is removed—meaning that each layer’s output only depends on the computations from the previous layer—the gradient must be propagated using the chain rule:

$$\frac{\partial u^r(a|k)}{\partial \theta} = \frac{\partial u^r(a|k)}{\partial h^{r,M}} \times \frac{\partial h^{r,M}}{\partial h^{r,M-1}} \times \frac{\partial h^{r,M-1}}{\partial h^{r,M-2}} \times \dots \times \frac{\partial h^{r,1}}{\partial v^r(a|k)} \times \frac{\partial v^r(a|k)}{\partial \theta} \quad (21)$$

If any intermediate gradient term becomes zero, the entire gradient vanishes, leading to failure in learning the weight matrices. Moreover, when $\theta^{r,M-1}$ is a matrix of which values of elements are very small, the instantaneous utility matrix of Res-RL U^r becomes:

$$U^r = h^{r,M-1} - J \times \ln 2 \otimes A \quad (22)$$

This formulation is equivalent to a Res-RL with only $M-1$ hidden layers. It can be concluded that increasing the number of hidden layers will not decrease the prediction accuracy.

3.3. Residual Directed Graph Convolutional Network Recursive logit model

Since Res-RL can only capture the *intersection cross-effect*, we formulate our model, Residual Directed Graph Convolutional Network Recursive logit model (ResDGCN-RL), by significantly modifying Res-RL by incorporating GNN.

3.3.1. Directed Graph Convolutional Network (DGCN)

Graph Convolutional Network (GCN) is widely used to process data with graph structures due to its ability to leverage both the feature of nodes and spatial relationships (Scarselli et al., 2008). However, traditional GCN assumes that the graph is undirected, which contradicts the nature of road networks, where links have distinct origins and destinations. Tong et al. (2020) proposed a Directed Graph Convolutional Network (DGCN) to take the directed graph feature into consideration by first-degree and second-order proximity.

First, we introduce GCN to establish key notations relevant to DGCN. The goal of GCN is to learn new features from the graph $G = \langle \mathcal{A}, \mathcal{V} \rangle$ with adjacency matrix A . The input of GCN is an $N \times D$ matrix X , where N is the number of nodes and D is the number of features. The output of GCN is an $N \times F$ matrix Z , where F is the learned representations.

For each hidden layer $h^{(m)}$:

$$h^{(m)} = \sigma(\tilde{D}^{-\frac{1}{2}} \tilde{A} \tilde{D}^{-\frac{1}{2}} h^{(m-1)} W^{(m)}) \quad \forall m \geq 1 \quad (23)$$

where σ is the activation function, the term $\tilde{A} = A + I$ where I is identity matrix to enforce self-loops and \tilde{D} is the degree matrix of \tilde{A} . $W^{(m)}$ is a learnable weight matrix of m -th hidden layer.

In DGCN, $\tilde{D}^{-\frac{1}{2}} \tilde{A} \tilde{D}^{-\frac{1}{2}}$ is replaced by First-order and Second-order proximity convolution which are defined as:

$$Z_F = \tilde{D}_F^{-\frac{1}{2}} \tilde{A}_F \tilde{D}_F^{-\frac{1}{2}} \quad (24)$$

$$Z_{S_{in}} = \tilde{D}_{S_{in}}^{-\frac{1}{2}} \tilde{A}_{S_{in}} \tilde{D}_{S_{in}}^{-\frac{1}{2}} \quad (25)$$

$$Z_{S_{out}} = \tilde{D}_{S_{out}}^{-\frac{1}{2}} \tilde{A}_{S_{out}} \tilde{D}_{S_{out}}^{-\frac{1}{2}} \quad (26)$$

where Z_F , $Z_{S_{in}}$ and $Z_{S_{out}}$ correspond to First-order, Second-order in-degree and out-degree proximity convolution respectively. The definition of adjacency matrix with self-loops and degree matrix, \tilde{D}_F , $\tilde{D}_{S_{in}}$, and $\tilde{D}_{S_{out}}$, remain consistent with those in GCN.

The First-order, Second-order proximity matrix is defined as:

$$A_F(i, j) = A_{i,j}^{\text{sym}} \quad (27)$$

$$A_{S_{in}}(i, j) = \sum_k \frac{A_{i,k} A_{j,k}}{\sum_v A_{v,k}} \quad (28)$$

$$A_{S_{\text{out}}}(i, j) = \sum_k \frac{A_{k,i}A_{k,j}}{\sum_v A_{k,v}} \quad (29)$$

where A^{sym} is the symmetric matrix of A .

Then, for each hidden layer $h^{(m)}$:

$$h^{(m)} = \text{softmax} \left(\text{Concat} \left(Z_F h^{(m-1)} W_1^{(m)}, \delta_1 Z_{S_{\text{in}}} h^{(m-1)} W_1^{(m)}, \delta_2 Z_{S_{\text{out}}} h^{(m-1)} W_1^{(m)} \right) \right) \quad \forall m \geq 1 \quad (30)$$

where where softmax is an activation function that transforms the input values into a probability distribution, ensuring that the elements sum to 1. Concat(\cdot) means matrix concatenation, and δ_1 and δ_2 are two learnable parameters to control the relative importance between different proximities.

3.3.2. Formulation of ResDGCN-RL

We draw inspiration from DGCN and propose a novel model named ResDGCN-RL. The framework of ResDGCN-RL is shown in figure 4. The proposed model processes adjacency and proximity matrices through DGCN layers with residual connections, generating the instantaneous utility matrix.

Specifically, The instantaneous utility of traveling from link k to a of ResDGCN-RL, denoted as $u^d(a|k)$, follows the same formulation as Res-RL:

$$u^d(a|k) = v^d(a|k) + g^d(a|k) + \epsilon(a) \quad (31)$$

where $v^d(a|k)$ and $g^d(a|k)$ are the residual component and the systematic component of $u^d(a|k)$, respectively.

The residual component matrix G^d with elements $G^d(k, a) = g^d(a|k)$ is learned via a modified DGCN to capture link cross-effect:

$$G^d = - \sum_{m=1}^M \text{ReLU} \left((\alpha Z_F + \beta Z_{S_{\text{in}}} + \gamma Z_{S_{\text{out}}}) h^{d,m-1} \theta^{r,m} \right) \otimes A \quad (32)$$

For the m -th hidden layer $h^{d,m}$:

$$h^{d,m} = h^{d,m-1} - \sum_{m'=1}^m \text{ReLU} \left((\alpha Z_F + \beta Z_{S_{\text{in}}} + \gamma Z_{S_{\text{out}}}) h^{d,m'-1} \theta^{r,m'} \right) \otimes A \quad (33)$$

where α, β and γ are three learnable parameters that reflect the contribution of $Z_F, Z_{S_{\text{out}}}$, and $Z_{S_{\text{in}}}$ explicitly and $\theta^{d,m}$ is the weight matrix in m -th hidden layer.

3.3.3. Property of ResDGCN-RL

Similar to Res-RL, ResDGCN-RL also has two properties which are interpretable weight matrix and skip-connection mechanism. However, while Res-RL is limited to capturing outgoing cross-effects, ResDGCN-RL extends this capability by incorporating multiple cross-effect patterns and explicitly exhibits the importance of them by parameters α, β , and γ .

To best understand the properties of the model, we first introduce the definitions of neighbor link pair, ingoing link pair and other cross-effect patterns.

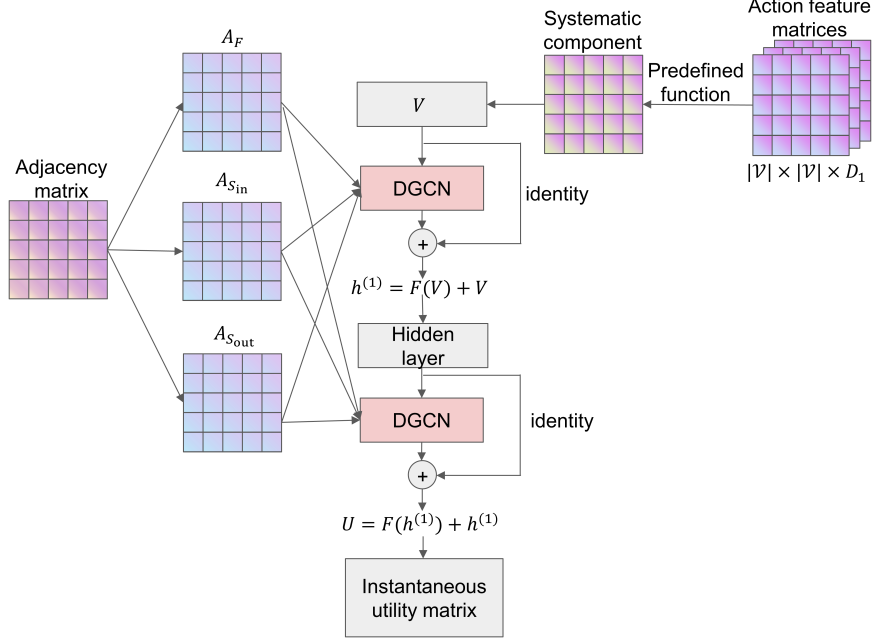


Figure 4: Framework of ResDGCN-RL. $F(\cdot)$ represents the modified DGCN propagation rule.

Neighbor link pair A neighbor link pair consists of two links that share a common node as one of their endpoints, either as a origin or a destination.

$$\{(u, v) \mid (u, v) \in \mathcal{V}\} \cup \{(v, w) \mid (v, w) \in \mathcal{V}\}$$

Ingoing link pair An ingoing link pair consists of two links that share a common node as their destinations.

$$\{(u, v) \mid (u, v) \in \mathcal{V}\} \cup \{(w, v) \mid (w, v) \in \mathcal{V}\}$$

Neighbor cross-effect The neighbor cross-effect refers to cross-effect between two actions that travel originated from links in a neighbor link pair.

Ingoing cross-effect The ingoing cross-effect refers to cross-effect between two actions that travel originated from links in a ingoing link pair.

Outgoing cross-effect The outgoing cross-effect refers to cross-effect between two actions that travel originated from links in a outgoing link pair.

In ResDGCN-RL, $\alpha^{\theta^{d,m}}(u, v)$, $\beta^{\theta^{d,m}}(u, v)$, and $\gamma^{\theta^{d,m}}(u, v)$ in m -th weight matrix explicitly present the *neighbor cross-effect*, *ingoing cross-effect* and *outgoing cross-effect* respectively. Figure 5 illustrates *neighbor link pair*, *outgoing link pair*, and *ingoing link pair*, where the cross-effect between links originate from links in these link pairs can be captured by first-order and second-order proximity matrices.

Consider a ResDGCN-RL with only one hidden layer,

$$u^d(a|k) = v^d(a|k) - \sum_i \left(\sum_j (\alpha Z_F(k, j) + \beta Z_{S_{in}}(k, j) + \gamma Z_{S_{out}}(k, j)) v^d(j, i) \theta^{d,0}(i, a) \right) \quad (34)$$

The partial derivate of $u^d(a|k)$ with respect to $v^d(a'|k')$ where k and k' form an *neighbor link pair* is:

$$\frac{\partial u^d(a|k)}{\partial v^d(a'|k')} = \alpha \theta^{d,0}(a', a) \quad (35)$$

By Second-order in-degree proximity matrix, the features of links are transferred between *ingoing link pair*. The partial derivate of $u^d(a|k)$ with respect to $v^d(a'|k')$ where k and k' form an *ingoing link pair* is:

$$\frac{\partial u^d(a|k)}{\partial v^d(a'|k')} = \beta \theta^{d,0}(a', a) \quad (36)$$

Similarly, by Second-order out-degree proximity matrix, the features of links are transferred between *outgoing link pair*. The partial derivate of $u^d(a|k)$ with respect to $v^d(a'|k')$ where k and k' form an *outgoing link pair* is:

$$\frac{\partial u^d(a|k)}{\partial v^d(a'|k')} = \gamma \theta^{d,0}(a', a) \quad (37)$$

Additionally, $(\alpha + \beta + \gamma) \theta^{d,0}(a', a)$ reflects the *intersection cross-effect*, which is the only pattern that Res-RL can capture. Therefore, the ability of capturing four different cross-effect patterns enhance its ability to capture travel behavior more comprehensively. Moreover, by increasing the number of hidden layers, the utility of a link can be influenced by farther links.

When the nonzero elements of weight matrix are in i -th row and j -th column where link i and link j form outgoing link pair, the ResDGCN-RL is the same as Res-RL. In this special case, ResDGCN-RL can capture the *intersection cross-effect* only. Since ResDGCN-RL generalizes Res-RL by incorporating additional cross-effect patterns, it is at least as effective as Res-RL, while offering greater flexibility in modeling complex cross-effect patterns.

3.4. Introduction of non-structured component: ResDGCN2-RL

Both Res-RL and ResDGCN-RL can only capture the structured features of links. Consequently, the deterministic utility of each link still depends on a predefined utility function. To overcome this limitation, this research proposes a method called ResDGCN2-RL, which is capable of capturing the non-structured correlation between features of each link. Figure 6 illustrates the framework of ResDGCN2-RL. The input consists of action feature matrices and link feature matrix. The structured component and non-structured component is computed via predefined function and DGCN respectively, and the rest of ResDGCN2-RL is the same as ResDGCN-RL.

The instantaneous utility of traveling from link k to a of ResDGCN2-RL is:

$$u^{d2}(a|k) = v^{d2}(a|k) + y^{d2}(a|k) + g^{d2}(a|k) + \epsilon(a) \quad (38)$$

where $y^{d2}(a|k)$, $v^{d2}(a|k)$, and $g^{d2}(a|k)$ are non-structured component, structured component, and residual component of $u^{d2}(a|k)$, respectively.

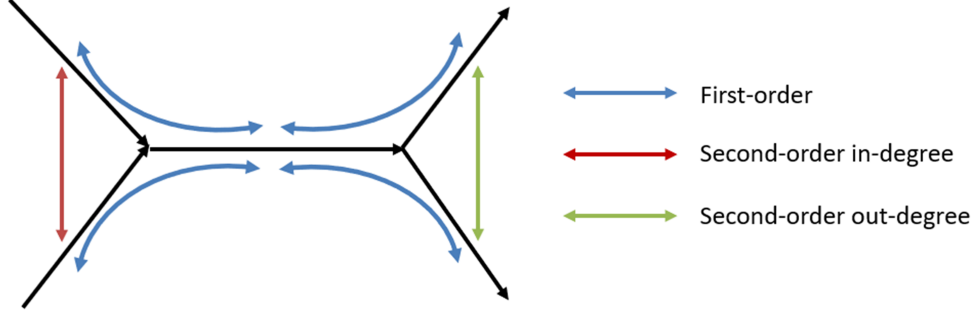


Figure 5: Illustration of First-order and Second-order adjacency

The non-structured component matrix Y^{d2} , where $Y^{d2}(k, a) = y^{d2}(a|k)$, is calculated by original DGCN introduced in section 3.3.1. The input layer is defined as $h^{d2,y,0} = X$, where X is link feature matrix with a size of $|V| \times D_2$. Here, D_2 denotes the number of link features.

For each hidden layer $h^{d2,y,m}$,

$$h^{d2,y,m} = \text{Concat} \left(Z_F h^{d2,y,m-1} \theta^{d2,y,m}, \alpha^y Z_{S_{in}} h^{d2,y,m-1} \theta^{d2,y,m}, \beta^y Z_{S_{out}} h^{d2,y,m-1} \theta^{d2,y,m} \right), \quad \forall m \geq 1 \quad (39)$$

The definition of Z_F , $Z_{S_{in}}$, and $Z_{S_{out}}$ is the same as equation (24), (25) and (26). α^y , and β^y are two learnable parameters to evaluate the impact of Second-order proximity convolution. $\theta^{d2,y,m}$ is a $3D^{m-1} \times D^m$ weight matrix where D^m is the number of new features of each link in m -th hidden layer.

The final output of DGCN for computing the non-structured component is given by:

$$Y^{d2} = h^{d2,y,M} \mathbf{1}_{3D^M \times |V|} \otimes A \quad (40)$$

where $\mathbf{1}_{3D^M \times |V|}$ is a matrix of ones with dimensions $3D^M \times |V|$.

The way to calculate residual component matrix G^{d2} with elements $G^{d2}(k, a) = G^{d2}(a|k)$ is very similar to ResDGCN-RL but replace the input V^d with $V^{d2} + Y^{d2}$.

$$G^{d2} = - \sum_{m=1}^M \text{ReLU} \left((\alpha^g Z_F + \beta^g Z_{S_{in}} + \gamma^g Z_{S_{out}}) h^{d2,g,m-1} \theta^{d2,g,m-1} \right) \otimes A \quad (41)$$

where ReLU is Rectified Linear Unit, a widely used activation function. $\theta^{d2,g,m-1}$ is an $|V| \times |V|$ weight matrix in m -th hidden layer.

The input layer of residual component $h^{d2,g,0}$ is the summation of structured component V^{d2} and non-structured component Y^{d2} :

$$h^{d2,g,0} = V^{d2} + Y^{d2} \quad (42)$$

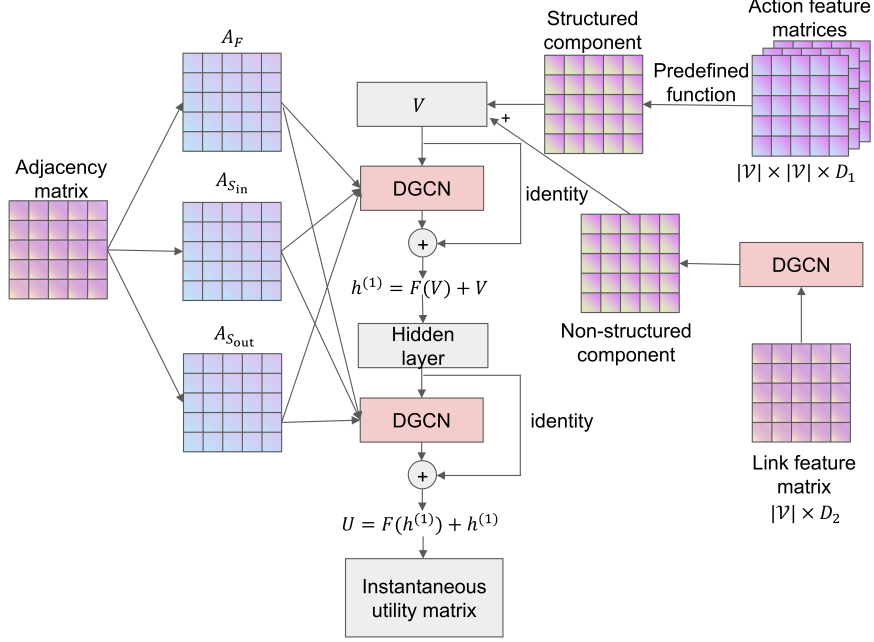


Figure 6: Framework of ResDGCN2-RL

The output of each hidden layer $h^{d2,g,m}$ is calculated by a modified DGCN with residual connection:

$$h^{d2,g,m} = h^{d2,g,m-1} - \sum_{m'=1}^m \text{ReLU}((\alpha Z_F + \beta Z_{S_{in}} + \gamma Z_{S_{out}}) h^{d,m-1} \theta^{d2,m}) \otimes A \quad (43)$$

$\forall m \geq 1$

When all weight matrices $\theta^{d2,y,m}$ ($\forall m \leq M$) are set to zero, ResDGCN2-RL reduces to ResDGCN-RL. This ensures that ResDGCN2-RL theoretically outperforms ResDGCN-RL, as it extends the latter by incorporating non-structured correlations, providing a more flexible and expressive representation of link utilities.

3.5. Loss function

In RL, the estimation method used is maximum log-likelihood estimation. The log-likelihood is defined as:

$$\text{LL} = \sum_{n=1}^N \sum_{l=1}^{l_n-1} \ln P^d(a_{l+1}^n | a_l^n) \quad (44)$$

where LL represents log-likelihood, N is the number of observed trajectories, l_n denotes the number of links in n -th trajectory and a_l^n refers to the l -th link in n -th trajectory.

To balance the trade-off between interpretability and prediction accuracy, we introduce a penalty coefficient λ into the loss function inspired by L2 regularization. The interpretability of a model is defined by:

$$\text{Interpretability} = - \sum_{m=1}^M \|\theta^{o,m}\|_2 \quad (45)$$

where o represents either r or d , distinguish Res-RL and ResDGCN-RL, respectively. $\|\cdot\|_2$ represents the Euclidean norm.

A lower interpretability value indicates that the instantaneous utility relies more on the systematic component and less on the residual component. This suggests that parameters within the systematic component carry more meaningful information, enabling better interpretation of feature importance (e.g., the value of time). Since standard RL does not incorporate a deep learning component, its interpretability is considered zero.

The loss function of Res-RL and ResDGCN-RL is formulated as:

$$\text{Loss} = -\text{LL} - \lambda \times \text{Interpretability} \quad (46)$$

A higher λ enhances interpretability at the cost of reduced prediction accuracy, whereas a lower λ prioritizes prediction performance over interpretability. The appropriate value of λ depends on the magnitude of features and the objective of the model. The optimal choice of λ depends on the scale of the features and the specific objective of the model. For instance, if the goal is to understand travel behavior to support urban planning decisions, a higher λ can be selected to emphasize interpretability. Conversely, if the primary focus is achieving high predictive accuracy, such as in traffic forecasting or route recommendation, setting $\lambda = 0$ would be more appropriate. Additionally, an intermediate λ value can be chosen to achieve a slight improvement in prediction accuracy while still maintaining a certain level of interpretability.

ResDGCN2-RL introduces a non-structured component to improve prediction accuracy. Therefore, the penalty term is omitted from its loss function, allowing the model to fully leverage non-structured feature.

For consistency in notation, throughout this paper, we use Res-RL ($M = m, \lambda = l$) to denote a Res-RL model with m hidden layers and a penalty coefficient of l . The same notation applies to ResDGCN-RL and ResDGCN2-RL.

4. Illustrative example

In this section, we present a small-scale illustrative example to demonstrate the properties and advantages of the proposed models in comparison with existing models. Note that a large-scale evaluation of the model will be conducted in a later section.

We use a simple toy network shown in figure 7, which is a typical network where the IIA property is important. Given a set of observed trip data, we estimate the models and analyze their results in detail. Specifically, we examine how the proposed model relaxes the IIA property by incorporating cross-effects between links and how the weight matrix explicitly captures these dependencies.

4.1. Scenario description

The network consists of five links and provides three alternative paths from link 0 to link 5, which are $0 \rightarrow 1 \rightarrow 3 \rightarrow 5$, $0 \rightarrow 1 \rightarrow 4 \rightarrow 5$, and $0 \rightarrow 2 \rightarrow 5$. These paths are labeled as path 1,

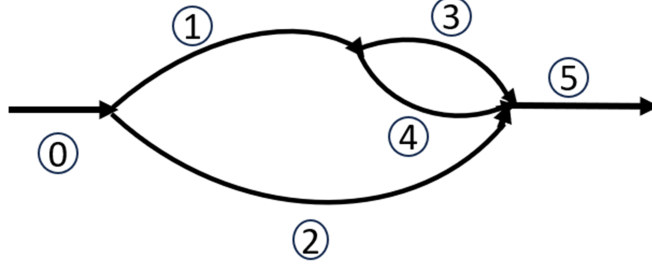


Figure 7: A very simple 3-path network for illustration

path 2, and path 3 respectively. The only feature considered for each link i is travel time t_i , and $t_1 = 90$, $t_2 = 100$, $t_3 = t_4 = 10$, $t_0 = t_5 = 0$. The training data is that 30% of travelers choose path 1, 30% of travelers choose path 2, and 40% of travelers choose path 3.

The observed travel time and training data are set to simulate real-world travel behavior. If the travel behavior is assumed to strictly follow MNL model, the probability of choosing each path is 33%. However, Paths 1 and 2 share a common sub-path $0 \rightarrow 1$, creating a strong correlation between them. As a result, their combined probability is slightly lower than the theoretical 66%, while path 3 gains a higher choosing probability due to the reduced competition from correlated alternatives.

4.2. Model specification

In this experiment, we use RL, RL with link size (RL-LS), Nested RL (NRL), Nested RL with link size (NRL-LS), Res-RL ($M = 1$), and ResDGCN-RL ($M = 1$) to explain the properties of our models. The instantaneous utility function of each model is formulated as follows:.

$$\mathbf{RL} \quad v^{\mathbf{RL}}(a|k) = \beta_t t_a$$

$$\mathbf{RL-LS} \quad v^{\mathbf{RL-LS}}(a|k) = \beta_t t_a + \beta_{LS} LS_a$$

$$\mathbf{NRL} \quad v^{\mathbf{NRL}}(a|k) = \frac{\beta_t t_a}{e^{\gamma t_a + \gamma_{LS} LS_a}}$$

$$\mathbf{NRL-LS} \quad v^{\mathbf{NRL-LS}}(a|k) = \frac{\beta_t t_a + \beta_{LS} LS_a}{e^{\gamma t_a + \gamma_{LS} LS_a}}$$

$$\mathbf{Res-RL} \quad v^{\mathbf{Res-RL}}(a|k) = \beta_t t_a + \ln 2$$

$$\mathbf{ResDGCN-RL} \quad v^{\mathbf{ResDGCN-RL}}(a|k) = \beta_t t_a$$

The link size feature of each link LS_i is computed using the RL model with parameter $\beta_t = -0.01$ which is used to address the IIA property. The key difference between NRL and RL is that the scale parameter in NRL is variable rather than constant. The constant term in the utility function of Res-RL is introduced to reduce the impact of residual component when θ is zero matrix. The initial training parameters are set to $\beta_t = -0.01$, with θ in both Res-RL and ResDGCN-RL initialized as a zero matrix. Additionally, the parameters $\alpha = \beta = \gamma$ are set to -1, while all other parameters are set to zero. The model is trained with a learning rate of 0.001 and a maximum of 10,000 iterations.

Table 1: Estimation results of RL and its variants

Model	β_t	β_{LS}	γ_t	γ_{LS}	log-likelihood	interpretability
RL	-0.010	-	-	-	-10.986	0
RL-LS	-0.010	-0.432	0	0	-10.889	0
NRL	-0.030	-	-0.001	0.153	-10.889	0
NRL-LS	-0.030	-0.001	-0.001	0.153	-10.889	0

Table 2: Estimation result of Res-RL

Model	β_t	log-likelihood	interpretability
Res-RL($M = 1, \lambda = 0$)	-0.062	-10.889	-0.056
Res-RL($M = 1, \lambda = 0.1$)	-0.105	-10.891	-0.027
Res-RL($M = 1, \lambda = 0.2$)	-0.214	-10.892	-0.015
Res-RL($M = 1, \lambda = 0.3$)	-0.216	-10.893	-0.011
Res-RL($M = 1, \lambda = 0.4$)	-0.222	-10.896	-0.010
Res-RL($M = 1, \lambda = 0.5$)	-0.289	-10.896	-0.008

4.3. Estimation result

Tables 1, 2, and 3 present the estimated parameters, log-likelihood, and interpretability for RL, its variants, Res-RL, and ResDGCN-RL. To further illustrate the advantages of these models, Table 4 provides the estimated choice probabilities, offering a more intuitive comparison of their prediction performance. Regardless of changes in model parameters, the RL model estimates that the choice probability for each path is 33%, which is obviously unrealistic. By introducing the link size feature, RL-LS can address this problem and the predicted choice probabilities match the observed data. However, when the travel times of links 3 and 4 are adjusted while keeping the total utility of all three paths unchanged, the estimated choice probability from the trained model remain the same. This result is incorrect because the correlation between paths 1 and 2 has changed. The reason for this erroneous prediction is that the link size feature is still influenced by the IIA assumption, preventing it from capturing changes in correlation across paths. NRL can also address this problem, but it suffers from strong assumptions. In contrast, Res-RL and ResDGCN-RL not only provide realistic estimated choice probabilities but also dynamically adjust the residual component in response to travel time changes, thereby generating varying choice probabilities that reflect the updated network conditions.

Furthermore, as shown in table 2 and 3, the predicted results of Res-RL and ResDGCN-RL match the observed data when the penalty coefficient is 0. With an increasing penalty coefficient, prediction accuracy decreases while interpretability improves.

Tables 5, 6, and 7 show how Res-RL($M = 1, \lambda = 0$) and ResDGCN-RL($M = 1, \lambda = 0$) relax the IIA property. For RL, $u(a|k)$ depends only on the link k and a , leading to identical total utilities for paths 1, 2, and 3. However, for Res-RL and ResDGCN-RL, $u(a|k)$ also depends on other actions and $g(a|k)$ plays a corrective role, ensuring that the total utilities of paths 1, 2, and 3 are no longer identical.

Table 3: Estimation result of ResDGCN-RL

Model	β_r	α	β	γ	log-likelihood	interpretability
ResDGCN-RL($M = 1, \lambda = 0$)	-0.031	-1.001	-1.002	-1.002	-10.889	-0.029
ResDGCN-RL($M = 1, \lambda = 0.1$)	-0.093	-1.001	-1.002	-1.002	-10.889	-0.014
ResDGCN-RL($M = 1, \lambda = 0.2$)	-0.062	-1.001	-1.004	-1.004	-10.891	-0.012
ResDGCN-RL($M = 1, \lambda = 0.3$)	-0.092	-1.001	-1.002	-1.002	-10.891	-0.008
ResDGCN-RL($M = 1, \lambda = 0.4$)	-0.076	-1.000	-1.001	-1.001	-10.894	-0.009
ResDGCN-RL($M = 1, \lambda = 0.5$)	-0.083	-1.000	-1.001	-1.001	-10.896	-0.008

Table 4: Estimated choice probability of different models

Model	Estimated choice probability		
	Path 1	Path 2	Path 3
True choice probability	30%	30%	40%
RL	33%	33%	33%
RL-LS	30%	30%	40%
NRL	30%	30%	40%
Res-RL($M = 1, \lambda = 0$)	30%	30%	40%
ResDGCN-RL($M = 1, \lambda = 0$)	30%	30%	40%

Table 5: Illustration of three-path choice scenario by using the estimated result of RL

k	a	$v(a k)$	$\exp(V(a))$	$P(a k)$
0	1	-0.9	1.81	0.66
0	2	-1	1	0.33
1	3	-0.1	1	0.50
1	4	-0.1	1	0.50

Table 6: Illustration of three-path choice scenario by using the estimated result of Res-RL($M = 1, \lambda = 0$)

k	a	$v(a k)$	$g(a k)$	$u(a k)$	$\exp(V(a))$	$P(a k)$
0	1	-4.866	-0.853	-5.719	1.078	0.6
0	2	-5.484	-0.567	-6.050	1	0.4
1	3	0.076	-0.693	-0.617	1	0.5
1	4	0.076	-0.693	-0.617	1	0.5

Table 7: Illustration of three-path choice scenario by using the estimated result of ResDGCN-RL($M = 1, \lambda = 0$)

k	a	$v(a k)$	$g(a k)$	$u(a k)$	$\exp(V(a))$	$P(a k)$
0	1	-2.771	-0.284	-3.055	1.465	0.6
0	2	-3.079	0.000	-3.079	1	0.4
1	3	-0.308	-0.003	-0.311	1	0.5
1	4	-0.308	-0.003	-0.311	1	0.5

4.4. Meaning of residual component in Res-RL

The weight matrix of Res-RL($M = 1, \lambda = 0$) is:

$$\theta^{r,1} = \begin{pmatrix} 0 & 0 & 0 & 0 & 0 & 0 \\ 0 & -0.026 & -0.031 & 0 & 0 & 0 \\ 0 & 0.023 & 0.028 & 0 & 0 & 0 \\ 0 & 0 & 0 & 0.005 & 0.005 & 0 \\ 0 & 0 & 0 & 0.005 & 0.005 & 0 \\ 0 & 0 & 0 & 0 & 0 & 0 \end{pmatrix} \quad (47)$$

From equation 47, we observe that the systematic utility of link 1 negatively influences the instantaneous utility of link 2. This means that as the travel time on link 1 increases, the instantaneous utility of link 2 increases. Additionally, the utilities of links 3 and 4 show a positive cross-effect, which is theoretically reasonable since these links share an overlapping link.

The weight matrix of ResDGCN-RL($M = 1, \lambda = 0$) is:

$$\theta^{d,1} = \begin{pmatrix} 0 & 0 & 0 & 0 & 0 & 0 \\ 0 & 0.019 & 0.022 & -3 \times 10^{-4} & -3 \times 10^{-4} & 0 \\ 0 & -2 \times 10^{-4} & -2 \times 10^{-4} & -3 \times 10^{-6} & -3 \times 10^{-6} & 0 \\ 0 & 0.001 & 0.001 & 0.001 & 0.001 & 0 \\ 0 & 0.001 & 0.001 & 0.001 & 0.001 & 0 \\ 0 & 0 & 0 & 0 & 0 & 0 \end{pmatrix} \quad (48)$$

Compared to the weight matrix in equation 47, the weight matrix of ResDGCN-RL contains more nonzero elements, indicating that ResDGCN-RL can capture much more complex cross-effect patterns between links. For Res-RL, only the cross-effects between links 1 and 2, as well as between links 3 and 4, can be captured. However, from the equation 48, it can be observed that in the case of ResDGCN-RL, cross-effects among all links from 1 to 4 can be captured.

5. Case study

In this section, we validate our models using a real-world travel dataset from Tokyo. First, we conduct a comparative analysis to compare three groups of models: (1) RL as the baseline, (2) NRL, and (3) our proposed models, including Res-RL and ResDGCN-RL. This comparison allows us to assess whether the proposed modules can further enhance performance beyond the existing RL variants. Additionally, we investigate whether the DGCN component can improve the performance of Res-RL. This can also be interpreted as an ablation study, as RL and Res-RL are simplification of ResDGCN-RL. We also evaluate model performance across different model depths and penalty coefficients.

5.1. Data description

In this section, we introduce the dataset used for model validation. The dataset is derived from an aggregated road network consisting of 1,196 links and 532 nodes, generated from vehicle trajectory data by Zhong et al. (2023) and originally provided by the Tokyo Metropolitan Government (shown in figure 8). The dataset comprises GPS vehicle positioning data from a specific area in Tokyo on August 18th, 2021, containing only major roads. The full dataset contains 105930 trips and 1516 origin-destination (OD) pairs, encompassing daily travel times and turn angles between links.

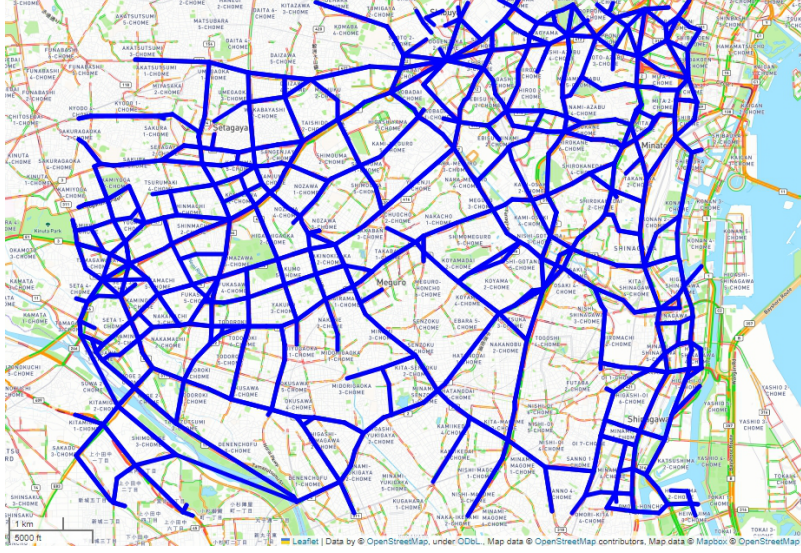


Figure 8: An aggregate road network. Source: © OpenStreetMap contributors, available under the Open Database License (ODbL).

5.2. Model specification

The utility function for traveling to link a from link k in RL, Res-RL, ResDGCN-RL, and ResDGCN2-RL is defined as:

$$v^{\text{RL}}(a|k) = \beta_{\text{TT}}\text{TT}_a + \beta_{\text{Spd}}\text{Spd}_a + \beta_{\text{RT}}\text{RT}_{a|k} + \beta_{\text{LC}} + \beta_{\text{uturn}}\text{uturn}_{a|k} \quad (49)$$

where TT_a and Spd_a represent the daily average travel time and speed of link a , respectively. $\text{RT}_{a|k}$ is a right-turn indicator (1 if the turn angle from k to a is between 40° and 170°), and $\text{uturn}_{a|k}$ is a U-turn indicator (1 if the turn angle is between 170° and 190°). β_{LC} is a link-independent constant penalizing routes with excessive intersections, while β_{uturn} is predefined as -100 to discourage U-turns. The parameters β_{TT} , β_{Spd} , β_{RT} , and β_{LC} are learnable.

The RL-LS model extends RL by incorporating the link size attribute:

$$v^{\text{RL-LS}}(a|k) = v^{\text{RL}}(a|k) + \beta_{\text{LS}}\text{LS}_a \quad (50)$$

where LS_a is computed using predefined parameters $\beta_{\text{TT}} = -1$, $\beta_{\text{Spd}} = -0.1$, $\beta_{\text{RT}} = -0.1$, and $\beta_{\text{LC}} = -0.1$.

For NRL and NRL-LS, a scale parameter μ_k is introduced:

$$\mu_k = \exp(\gamma_{\text{TT}}\text{TT}_a + \gamma_{\text{Spd}}\text{Spd}_a + \gamma_{\text{LS}}\text{LS}_a) \quad (51)$$

and the utility functions are given by:

$$v^{\text{NRL}}(a|k) = \frac{1}{\mu_k}v^{\text{RL}}(a|k), \quad v^{\text{NRL-LS}}(a|k) = \frac{1}{\mu_k}v^{\text{RL-LS}}(a|k) \quad (52)$$

To evaluate model performance, 30% of the complete dataset is allocated for validation. The models are trained using the Stochastic Gradient Descent (SGD) algorithm with a learning rate

of 10^{-6} . All trainable parameters are initialized following a predefined scheme. The systematic component parameters, including β_{TT} , β_{Spd} , β_{RT} , and β_{LC} , are set to -1.0 to ensure a reasonable starting point for optimization. The hidden layer parameters of the residual component are initialized as zero matrices, meaning that there is no cross-effect between links at the beginning of training. The training process is limited to a maximum of 500 iterations. The computational cost is primarily determined by model depth. For instance, training a model with two hidden layers requires approximately 8 hours.

Apart from log-likelihood, we also use average choice probability to represent prediction accuracy, which is defined as:

$$\text{average choice probability} = \frac{\sum_{n=1}^N \prod_{l=1}^{l_n-1} P^d(a_{l+1}^n | a_l^n)}{N} \quad (53)$$

The notation in equation 53 remains consistent with the previous sections.

5.3. Estimation result

Table 8: Estimation result of RL, variants of RL

Parameter	RL	RL-LS	NRL	NRL-LS
β_{TT}	-1.674	-1.432	-0.668	-0.656
β_{Spd}	-0.842	-0.553	-0.097	-0.053
β_{RT}	0.602	0.260	-0.216	-0.225
β_{LC}	-1.840	-1.264	-0.673	-0.718
β_{LS}	–	-0.905	–	-0.142
γ_{TT}	–	–	-0.069	-0.076
γ_{Spd}	–	–	-0.135	-0.159
γ_{LS}	–	–	-0.109	-0.110
log-likelihood	-9604.964	-9009.576	-8526.220	-8515.802
average choice probability	87.852%	87.450%	88.295%	88.298%

Table 9: Estimation result of Res-RL

Parameter	Res-RL($M = 1, \lambda = 0$)	Res-RL($M = 2, \lambda = 0$)	Res-RL($M = 2, \lambda = 2$)
β_{TT}	-1.031	-1.017	-1.224
β_{Spd}	-0.951	-0.968	-0.001
β_{RT}	-0.931	-0.951	0.676
β_{LC}	-1.004	-1.002	-1.036
log-likelihood	-2092.477	-1848.621	-7166.138
interpretability	-0.480	-0.640	-0.105
average choice probability	96.424%	96.741%	90.887%

Table 10: Estimation result of ResDGCN-RL

Parameter	ResDGCN-RL($M = 1, \lambda = 0$)	ResDGCN-RL($M = 2, \lambda = 0$)	ResDGCN-RL($M = 2, \lambda = 2$)
β_{TT}	-1.031	-1.061	-1.639
β_{Spd}	-0.943	-0.970	-0.746
β_{RT}	-0.957	-0.965	0.281
β_{LC}	-1.060	-1.014	-1.290
α	-0.169	-0.183	-0.314
β	-0.096	-0.273	-0.683
γ	-0.376	-0.337	-0.728
log-likelihood	-2002.710	-1843.906	-6223.100
interpretability	-1.051	-0.624	-0.036
average choice probability	96.511%	96.539%	90.359%

Table 11: Estimation result of ResDGCN2-RL

Parameter	ResDGCN2-RL ($M = 2$)
β_{TT}	-1.227
β_{Spd}	-0.855
β_{RT}	-0.991
β_{LC}	-1.037
α^y	-0.010
β^y	-0.023
α^g	-0.178
β^g	-0.241
γ	-0.351
log-likelihood	-1821.048
average choice probability	96.899%

Tables 8 shows the estimation result of RL and its variants by using real-world dataset, indicates that the variants of RL do not significantly improve the prediction accuracy of RL itself. Tables 9, 10, and 11 show the estimation result of Res-RL, ResDGCN-RL, and ResDGCN2-RL, respectively, indicate Res-RL, ResDGCN-RL, and ResDGCN2-RL are highly effective in enhancing prediction accuracy. By comparing the prediction results of ResDGCN2-RL, ResDGCN-RL, and Res-RL with the same number of layers, we find that the DGCN component does not significantly improve the model's accuracy.

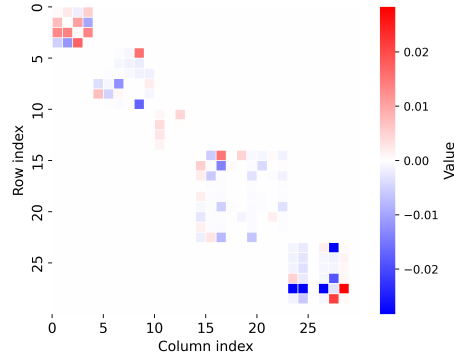


Figure 9: Heatmap of the weight matrix for the first hidden layer of Res-RL(M=2, $\lambda=0$)

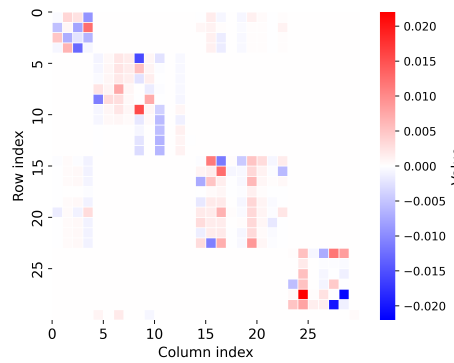


Figure 10: Heatmap of the weight matrix for the first hidden layer of ResDGCN-RL(M=2, $\lambda=0$)

Figure 9 and figure 10 further support the conclusion drawn in Section 4, showing that the weight matrix of Res-RL captures *intersection cross-effect* and can be reflected by weight matrix, while ResDGCN-RL can capture much more complex cross-effect patterns.

Figure 11 illustrates an example of discrepancies between the actual chosen route and the most probable route predicted by different models. Such discrepancies are more frequent when the route is short. Notably, the predicted routes of RL and hybrid models with high penalty coefficients are almost identical.

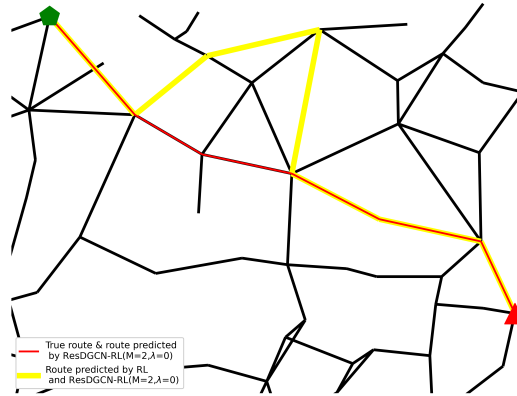


Figure 11: The actual chosen route and the most probable route predicted by different models

5.4. Sensitivity analysis

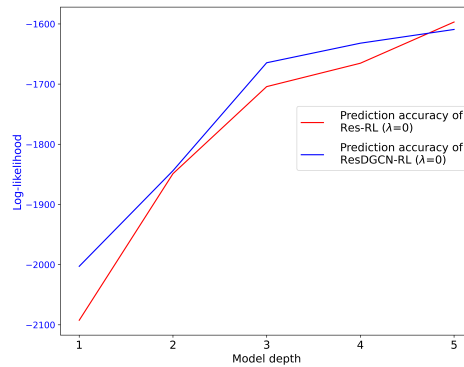


Figure 12: Sensitivity analysis on model depth

Figure 12 presents the performance of Res-RL and ResDGCN-RL at different model depths. As the number of hidden layers increases, the prediction accuracy of the models improves. When $M \geq 3$, the changes are not very significant, but the training time and memory requirements grow significantly. Therefore, a model with two to three layers strikes a balance between accuracy and computational efficiency.

Figure 13 presents the changes in log-likelihood and interpretability for Res-RL and ResDGCN-RL under different penalty coefficients. Both models exhibit similar trends: as λ increases, log-likelihood improves, approaching the predictive accuracy of RL, while interpretability decreases, tending towards zero. Notably, the rate of change diminishes at higher λ values. Additionally, it is important to note that due to differences in model structure, the interpretability of Res-RL and ResDGCN-RL cannot be directly compared. Moreover, their sensitivity to the penalty coefficient also differs.

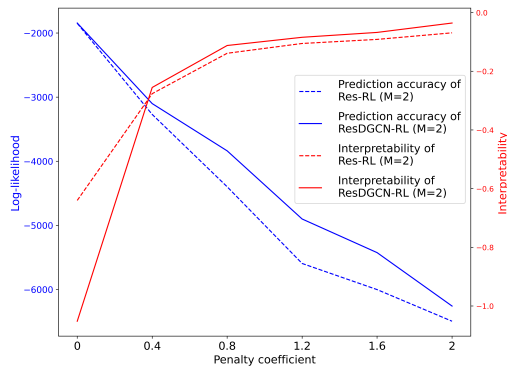


Figure 13: Sensitivity analysis on penalty coefficient

6. Conclusion and discussion

In this study, hybrid route choice models, namely ResDGCN-RL and ResDGCN2-RL, that combines interpretable logit-type model and efficient graph neural networks are proposed, which improve upon RL by decomposing the deterministic term in the utility function into a systematic component, computed using a pre-defined utility function, and a residual component, learned via deep learning techniques. To enhance model stability, skip connections inspired by ResNet are employed to mitigate vanishing and exploding gradient issues, ensuring that deeper models consistently enhance performance. Additionally, given the importance of interpretability in route choice modeling, we introduce a regularization-based loss function to balance the trade-off between interpretability and prediction accuracy.

To evaluate the effectiveness of the proposed models, we conducted experiments on a simple three-path network and a real-world trajectory dataset from Tokyo. The results demonstrate that the proposed models outperform RL and its variants in terms of prediction accuracy. Mathematical analysis confirms that Res-RL only captures *intersection cross-effect*, whereas ResDGCN-RL and ResDGCN2-RL are capable of modeling broader cross-effect patterns. Although the improvements of ResDGCN-RL and ResDGCN2-RL over Res-RL in terms of quantitative accuracy were not very large, ResDGCN-RL and ResDGCN2-RL captured the network property reasonably.

Despite these improvements, the proposed models have certain limitations. First, GCN capture only local feature correlations between adjacent nodes, limiting their ability to model global dependencies, which are critical for route choice modeling. Second, the computational complexity remains high due to the large weight matrix, posing challenges for large-scale applications. Third, the models lack generalization ability, as they are trained on a fixed road network and cannot be directly transferred to other networks.

Future research could address these limitations by integrating attention mechanisms (Vaswani et al., 2017) to capture long-range dependencies in road networks, developing parameter-efficient architectures to reduce computational costs, and exploring domain adaptation techniques to improve model generalization ability across different network structures.

Acknowledgment

The data is provided by Tokyo Metropolitan Government through their project 'offering of several datasets on mobility and transportation in Tokyo 2020 Games'. Map data copyrighted OpenStreetMap contributors and available from <https://www.openstreetmap.org>.

CRedit author contribution statement

Ma Yuxun: Conceptualization; Methodology; Data curation; Formal analysis; Investigation; Validation; Visualization; Writing - original draft. **Toru Seo:** Conceptualization; Data curation; Funding acquisition; Project administration; Resources; Supervision; Writing - review & editing.

Declaration of competing interest

The authors declare that there are no known competing interests.

Declaration of generative AI and AI-assisted technologies in the writing process

During the preparation of this work, the authors used GPT-4o for a grammatical proofreading purpose. After using this tool/service, the authors reviewed and edited the content as needed and take full responsibility for the content of the publication.

References

- Bai, L., Yao, L., Li, C., Wang, X., and Wang, C. (2020). Adaptive graph convolutional recurrent network for traffic forecasting. *Advances in neural information processing systems*, 33:17804–17815.
- Bekhor, S. and Prashker, J. (2001). Stochastic user equilibrium formulation for generalized nested logit model. *Transportation Research Record*, 1752(1):84–90.
- Ben-Akiva, M., Scott, M., and Bekhor, S. (2004). Route choice models. human behaviour and traffic networks. *Springer Berlin Heidelberg*, pages 23–45.
- Ben-Akiva, M. E. and Lerman, S. R. (1985). *Discrete choice analysis: theory and application to travel demand*, volume 9. MIT press.
- Bovy, P. H., Bekhor, S., and Prato, C. G. (2008). The factor of revisited path size: Alternative derivation. *Transportation Research Record*, 2076(1):132–140.
- Cascetta, E., Nuzzolo, A., Russo, F., and Vitetta, A. (1996). A modified logit route choice model overcoming path overlapping problems. specification and some calibration results for interurban networks. In *Transportation and Traffic Theory. Proceedings of The 13th International Symposium On Transportation And Traffic Theory, Lyon, France, 24-26 July 1996*.
- Cheng, S., Lu, F., Peng, P., and Wu, S. (2018). Short-term traffic forecasting: An adaptive st-knn model that considers spatial heterogeneity. *Computers, Environment and Urban Systems*, 71:186–198.
- Dia, H. and Panwai, S. (2007). Modelling drivers' compliance and route choice behaviour in response to travel information. *Nonlinear Dynamics*, 49:493–509.
- Dong, G., Kweon, Y., Park, B. B., and Boukhechba, M. (2022). Utility-based route choice behavior modeling using deep sequential models. *Journal of big data analytics in transportation*, 4(2):119–133.
- Du, H., Leng, S., Wu, F., Chen, X., and Mao, S. (2020). A new vehicular fog computing architecture for cooperative sensing of autonomous driving. *IEEE Access*, 8:10997–11006.
- Fosgerau, M., Frejinger, E., and Karlstrom, A. (2013). A link based network route choice model with unrestricted choice set. *Transportation Research Part B: Methodological*, 56:70–80.
- Fouladgar, M., Parchami, M., Elmasri, R., and Ghaderi, A. (2017). Scalable deep traffic flow neural networks for urban traffic congestion prediction. In *2017 international joint conference on neural networks (IJCNN)*, pages 2251–2258. IEEE.

- Ghahremannezhad, H., Shi, H., and Liu, C. (2022). Real-time accident detection in traffic surveillance using deep learning. In *2022 IEEE international conference on imaging systems and techniques (IST)*, pages 1–6. IEEE.
- Gumbel, E. (1958). Statistics of extremes.
- Hagenauer, J. and Helbich, M. (2017). A comparative study of machine learning classifiers for modeling travel mode choice. *Expert Systems with Applications*, 78:273–282.
- Han, Y., Pereira, F. C., Ben-Akiva, M., and Zegras, C. (2020). A neural-embedded choice model: Tastenet-mnl modeling taste heterogeneity with flexibility and interpretability. *arXiv preprint arXiv:2002.00922*.
- He, K., Zhang, X., Ren, S., and Sun, J. (2016). Identity mappings in deep residual networks. In *Computer Vision—ECCV 2016: 14th European Conference, Amsterdam, The Netherlands, October 11–14, 2016, Proceedings, Part IV 14*, pages 630–645. Springer.
- He, S., Luo, Q., Du, R., Zhao, L., He, G., Fu, H., and Li, H. (2023). Stgc-gnns: A gnn-based traffic prediction framework with a spatial-temporal granger causality graph. *Physica A: Statistical Mechanics and its Applications*, 623:128913.
- Hu, X., Zhao, C., and Wang, G. (2020). A traffic light dynamic control algorithm with deep reinforcement learning based on gnn prediction. *arXiv preprint arXiv:2009.14627*.
- Lai, X., Fu, H., Li, J., and Sha, Z. (2019). Understanding drivers’ route choice behaviours in the urban network with machine learning models. *IET Intelligent Transport Systems*, 13(3):427–434.
- Lee, C., Ran, B., Yang, F., and Loh, W.-Y. (2010). A hybrid tree approach to modeling alternate route choice behavior with online information. *Journal of Intelligent Transportation Systems*, 14(4):209–219.
- Li, X.-y., Li, X.-m., Yang, L., and Li, J. (2018). Dynamic route and departure time choice model based on self-adaptive reference point and reinforcement learning. *Physica A: Statistical Mechanics and its Applications*, 502:77–92.
- Liang, X., Du, X., Wang, G., and Han, Z. (2019). A deep reinforcement learning network for traffic light cycle control. *IEEE Transactions on Vehicular Technology*, 68(2):1243–1253.
- Lu, H., Huang, D., Song, Y., Jiang, D., Zhou, T., and Qin, J. (2020). St-trafficnet: A spatial-temporal deep learning network for traffic forecasting. *Electronics*, 9(9):1474.
- Lu, Z., Lv, W., Xie, Z., Du, B., and Huang, R. (2019). Leveraging graph neural network with lstm for traffic speed prediction. In *2019 IEEE SmartWorld, Ubiquitous Intelligence & Computing, Advanced & Trusted Computing, Scalable Computing & Communications, Cloud & Big Data Computing, Internet of People and Smart City Innovation (SmartWorld/SCALCOM/UIC/ATC/CBDCOM/IOP/SCI)*, pages 74–81. IEEE.
- Ma, X., Tao, Z., Wang, Y., Yu, H., and Wang, Y. (2015). Long short-term memory neural network for traffic speed prediction using remote microwave sensor data. *Transportation Research Part C: Emerging Technologies*, 54:187–197.
- Mai, T., Bastin, F., and Frejinger, E. (2018). A decomposition method for estimating recursive logit based route choice models. *EURO Journal on Transportation and Logistics*, 7(3):253–275.
- Mai, T., Fosgerau, M., and Frejinger, E. (2015). A nested recursive logit model for route choice analysis. *Transportation Research Part B: Methodological*, 75:100–112.
- McFadden, D. and Train, K. (2000). Mixed mnl models for discrete response. *Journal of applied Econometrics*, 15(5):447–470.
- Phan, D. T., Vu, H. L., and Currie, G. (2022). Attentionchoice: Discrete choice modelling supported by a deep learning attention mechanism. Available at SSRN 4305637.
- Politis, I., Georgiadis, G., Kopsacheilis, A., Nikolaidou, A., Sfyri, C., and Basbas, S. (2023). A route choice model for the investigation of drivers’ willingness to choose a flyover motorway in greece. *Sustainability*, 15(5):4614.
- Prashker, J. N. and Bekhor, S. (2000). Congestion, stochastic, and similarity effects in stochastic: User-equilibrium models. *Transportation Research Record*, 1733(1):80–87.
- Scarselli, F., Gori, M., Tsoi, A. C., Hagenbuchner, M., and Monfardini, G. (2008). The graph neural network model. *IEEE transactions on neural networks*, 20(1):61–80.
- Schmid, B., Becker, F., Molloy, J., Axhausen, K. W., Lüdering, J., Hagen, J., and Blome, A. (2022). Modeling train route decisions during track works. *Journal of Rail Transport Planning & Management*, 22:100320.
- Siffringer, B., Lurkin, V., and Alahi, A. (2020). Enhancing discrete choice models with representation learning. *Transportation Research Part B: Methodological*, 140:236–261.
- Singh, D., Zaman, M. M., White, L., et al. (2011). Modeling of 85th percentile speed for rural highways for enhanced traffic safety. Technical report, Oklahoma. Dept of Transportation.
- Song, C., Lin, Y., Guo, S., and Wan, H. (2020). Spatial-temporal synchronous graph convolutional networks: A new framework for spatial-temporal network data forecasting. In *Proceedings of the AAAI conference on artificial intelligence*, volume 34, pages 914–921.
- Tang, J., Chen, X., Hu, Z., Zong, F., Han, C., and Li, L. (2019). Traffic flow prediction based on combination of support vector machine and data denoising schemes. *Physica A: Statistical Mechanics and its Applications*, 534:120642.
- Thaduri, A., Polepally, V., and Vodithala, S. (2021). Traffic accident prediction based on cnn model. In *2021 5th International conference on intelligent computing and control systems (ICICCS)*, pages 1590–1594. IEEE.
- Tong, Z., Liang, Y., Sun, C., Rosenblum, D. S., and Lim, A. (2020). Directed graph convolutional network. *arXiv*

- preprint *arXiv:2004.13970*.
- Tribby, C. P., Miller, H. J., Brown, B. B., Werner, C. M., and Smith, K. R. (2017). Analyzing walking route choice through built environments using random forests and discrete choice techniques. *Environment and Planning B: Urban Analytics and City Science*, 44(6):1145–1167.
- Vaswani, A., Shazeer, N., Parmar, N., Uszkoreit, J., Jones, L., Gomez, A. N., Kaiser, Ł., and Polosukhin, I. (2017). Attention is all you need. *Advances in neural information processing systems*, 30.
- Vidhate, D. A. and Kulkarni, P. (2017). Cooperative multi-agent reinforcement learning models (cmrlm) for intelligent traffic control. In *2017 1st International Conference on Intelligent Systems and Information Management (ICISIM)*, pages 325–331. IEEE.
- Wang, J., Wu, N., and Zhao, W. X. (2021). Personalized route recommendation with neural network enhanced search algorithm. *IEEE Transactions on Knowledge and Data Engineering*, 34(12):5910–5924.
- Wei, F., Ma, S., and Jia, N. (2014). A day-to-day route choice model based on reinforcement learning. *Mathematical Problems in Engineering*, 2014(1):646548.
- Wong, M. and Farooq, B. (2021). Reslogit: A residual neural network logit model for data-driven choice modelling. *Transportation Research Part C: Emerging Technologies*, 126:103050.
- Wong, M., Farooq, B., and Bilodeau, G.-A. (2018). Discriminative conditional restricted boltzmann machine for discrete choice and latent variable modelling. *Journal of choice modelling*, 29:152–168.
- Xiang, J. and Chen, Z. (2015). Adaptive traffic signal control of bottleneck subzone based on grey qualitative reinforcement learning algorithm. In *international conference on pattern recognition applications and methods*, volume 2, pages 295–301. SCITEPRESS.
- Xie, Q., Guo, T., Chen, Y., Xiao, Y., Wang, X., and Zhao, B. Y. (2020). Deep graph convolutional networks for incident-driven traffic speed prediction. In *Proceedings of the 29th ACM international conference on information & knowledge management*, pages 1665–1674.
- Xu, T., Xu, Y., Wang, D., Chen, S., Zhang, W., and Feng, L. (2020). Path planning for autonomous articulated vehicle based on improved goal-directed rapid-exploring random tree. *Mathematical Problems in Engineering*, 2020(1):7123164.
- Yai, T., Iwakura, S., and Morichi, S. (1997). Multinomial probit with structured covariance for route choice behavior. *Transportation Research Part B: Methodological*, 31(3):195–207.
- Yamamoto, T., Kitamura, R., and Fujii, J. (2002). Drivers’ route choice behavior: analysis by data mining algorithms. *Transportation Research Record*, 1807(1):59–66.
- Yang, H., Kitamura, R., Jovanis, P. P., Vaughn, K. M., and Abdel-Aty, M. A. (1993). Exploration of route choice behavior with advanced traveler information using neural network concepts. *Transportation*, 20:199–223.
- Zhang, W. and He, R. (2014). Dynamic route choice based on prospect theory. *Procedia-Social and Behavioral Sciences*, 138:159–167.
- Zhao, Z. and Liang, Y. (2023). A deep inverse reinforcement learning approach to route choice modeling with context-dependent rewards. *Transportation Research Part C: Emerging Technologies*, 149:104079.
- Zhong, H., Seo, T., Nakanishi, W., Yasuda, S., Asakura, Y., and Iryo, T. (2023). Generation of aggregated road network by vehicle trajectory data. *EU Science Hub*, page 50.
- Zhong, T., Xu, Z., and Zhou, F. (2021). Probabilistic graph neural networks for traffic signal control. In *ICASSP 2021-2021 IEEE International Conference on Acoustics, Speech and Signal Processing (ICASSP)*, pages 4085–4089. IEEE.
- Zou, Y., Ding, L., Zhang, H., Zhu, T., and Wu, L. (2022). Vehicle acceleration prediction based on machine learning models and driving behavior analysis. *applied sciences*, 12(10):5259.